PNAS RESEARCH ARTICLE | EVOLUTION

High-resolution single-cell analyses reveal evolutionary constraints and evolvability of sexual circuits in *Drosophila*

Justin T. Walsh[a,1,2], Ian P. Junker[a,3], Yu-Chieh David Chen[b,4], Yen-Chung Chen[b], Helena Gifford[a], Dawn S. Chen[a], and Yun Ding[a,1]

Affiliations are included on p. 10.

Edited by Michelle N. Arbeitman, Florida State University, Tallahassee, FL; received June 23, 2025; accepted October 9, 2025 by Editorial Board Member John R. Carlson

Understanding how the cellular and molecular composition of neural circuits evolves to generate species-specific behaviors remains a major challenge in evolutionary biology and neuroscience. The remarkable diversity of male sexual behaviors among *Drosophila* species, despite their recent divergence, offers an excellent model for addressing this question. Here, by harnessing single-cell transcriptomics of the sexual circuits labeled by the sex determination gene *doublesex* (*dsx*) at high resolution, we delineated 84 molecularly distinct *dsx*+ cell types, each mapped to anatomically and functionally defined *dsx*+ neural populations. Our findings revealed a largely conserved cellular architecture, with minimal evolutionary gain or loss of cell types across four *Drosophila* species. A detailed comparison between *Drosophila melanogaster* (*D. melanogaster*) and *D. yakuba* uncovered pervasive heterogeneity in transcriptomic divergence among *dsx*+ cell types. While core cell type identities—defined by the sex determination gene *fruitless* (*fru*), neurotransmitters, monoamines, and transcription factors—remain highly conserved, we observed striking evolutionary turnover in neuropeptide signaling pathways in a highly cell-type-specific manner, underscoring the role of functional reconfiguration of conserved circuits in behavioral evolution. Further investigation of sex differences in *dsx*+ neurons revealed that male-specific cell types are not more evolutionarily divergent than sex-unbiased ones. Finally, we developed an interactive web resource for data access and characterized marker gene combinations enabling cell-type-specific labeling. Overall, our study provides insights into how neural circuits evolve to encode behavioral diversity and establishes a high-resolution framework for understanding the cellular basis of behavioral adaptation.

neural circuit evolution | behavioral evolution | single-cell transcriptomics | evolution of cell types | neuropeptide signaling

Significance

How do nervous systems evolve to generate the extraordinary diversity of animal behaviors? We addressed this question by investigating how neural circuits evolve in fruit fly species with divergent sexual behaviors such as courtship. Using single-cell transcriptomics and anatomical mapping, we defined 84 neuron types and examined how their identities and gene expression have changed across species. We found that each neuron type follows a distinct evolutionary trajectory. While neuron types and core molecular properties are highly conserved, neuropeptide signaling genes—which modulate circuit functional connectivity rather than structural wiring—exhibit striking, cell-type-specific evolutionary turnover. Our findings indicate that fine-scale molecular alterations within conserved neural architectures may underlie the evolutionary diversification of behaviors.

Even among closely related species, behaviors may vary drastically, and this behavioral variation largely arises from evolutionary changes in the structure and function of the underlying homologous neural circuits (1, 2). These changes can occur through the presence and absence of specific cell types, the abundance of a particular cell type, or gene expression that influences neuron anatomy and physiology. Facilitated by the unprecedented capacity of single-cell RNA sequencing (scRNA-seq) to define molecular cell types, recent comparative studies have begun to shed light on conserved and divergent cell types across species and taxa (e.g., refs. 3–6). However, existing studies often focus on distantly related species and/or have limited resolution to capture fine-scale changes in cell types. Particularly, since the basic cellular organization of the nervous system tends to be largely conserved among closely related species (7), subtle changes in the nervous system may result in major behavioral differences but go undetected in existing datasets. With the exception of a few relatively simple organisms (8), it remains unclear how much neuronal cell types differ among related species with divergent behaviors at a fine-grained level. Furthermore, it is unclear whether certain cell types exhibit greater divergence across species and how gene expression evolves at the level of individual cell types.

Drosophila species, with their rich behavioral diversity and experimental accessibility, serve as a powerful system to study behavioral evolution through species comparisons (2, 9–13). *Drosophila* sexual behaviors present a unique opportunity as the genes and neural circuits underlying these behaviors have been well studied in the model species *Drosophila melanogaster* (14, 15) and these behaviors have rapidly diversified across species (16–18). For example, *Drosophila* males perform complex and diversified courtship rituals such as singing a species-specific courtship song by vibrating their wings (17). Species also vary in their responses to sensory cues that are visual, auditory, and chemosensory (18). These sexual behaviors are orchestrated by two key transcription factors in the sex determination

The authors declare no competing interest.

This article is a PNAS Direct Submission. M.N.A. is a guest editor invited by the Editorial Board.

[1]To whom correspondence may be addressed. Email: juswalsh@sas.upenn.edu or yding19@sas.upenn.edu.

[2]Present address: Department of Biology, Holy Family University, Philadelphia, PA 19114.

[3]Present address: Department of Biological and Biomedical Sciences, Vanderbilt University, Nashville, TN 37232.

[4]Present address: Department of Biology, Temple University, Philadelphia, PA 19122.

This article contains supporting information online at https://www.pnas.org/lookup/suppl/doi:10.1073/pnas.2516083122/-/DCSupplemental.

Published November 17, 2025.

pathway: *dsx* and *fru*. The *dsx* gene is spliced into sex-specific isoforms that regulate the development and function of sexual circuits (14). Approximately 700 to 800 *dsx*+ neurons, representing about 1% of the adult male central nervous system, are distributed in anatomically and functionally distinct neuronal clusters. For instance, the male-specific TN1 cluster in the ventral nerve cord (VNC) is a group of motor patterning neurons responsible for generating courtship song (19); the sexually dimorphic pC1 cluster in the brain integrates sensory cues and contains functionally heterogeneous populations that encode sexual and aggressive states (20, 21). Given the expanding knowledge of their roles in sexual behaviors–which evolve rapidly across species–*dsx*+ neurons provide an excellent inroad for uncovering the cellular and molecular mechanisms underlying the evolution of complex behaviors and species-specific adaptations. Indeed, we have previously linked the lineage-specific loss of a major type of courtship song called sine song in *Drosophila yakuba* to the loss of a neuronal subtype within the TN1 cluster (11).

In this study, we overcome the common challenge of achieving sufficient cellular resolution in comparative scRNA-seq studies by profiling genetically labeled *dsx*+ neurons across *Drosophila* species. This effort resulted in a scRNA-seq atlas comprising 46,922 *dsx*+ neurons in adult males, with each *dsx*+ neuron represented an average of 64 times. The dataset included four species within the *D. melanogaster* subgroup: *D. melanogaster*, *D. yakuba*, *D. santomea*, and *D. teissieri*—a group of closely related species that exhibit a wide range of differences in sexual behaviors and are emerging models for comparative studies of the nervous system and behavior (9–11, 22, 23). In total, we molecularly defined 84 cell types, all systematically mapped to and hierarchically organized by known *dsx*+ neuronal clusters, providing a comprehensive characterization of cellular diversity within this neuronal population of broad interest. We found that sexual circuits evolve through widespread cell-type-specific gene expression changes, particularly in neuropeptide signaling genes, on top of a largely conserved organization in cell types, sex identity, and neurotransmitter properties. We also generated a scRNA-seq dataset in adult *D. melanogaster* females to characterize female *dsx*+ cell types and explore the relationship between species divergence and sex differences. Finally, we compiled a list of marker gene combinations that uniquely target each cell type and hosted our datasets on a Shiny app interface that allows user-defined tasks such as gene expression inquiries and molecular marker detection across cell types, species, and sexes. Altogether, our study offers both insights and useful resources for understanding and dissecting the function and evolution of neural circuits.

Results

High-Resolution Characterization of Cell Type Diversity within *dsx*+ Neurons. We genetically labeled *dsx*+ neurons using CRISPR/Cas9-mediated genome editing (11) and fluorescently sorted them from adult male brains and VNCs of four *Drosophila* species that diverged within the past 12 My (24) (Fig. 1*A*). In total, we generated three replicates for *D. melanogaster* and *D. yakuba,* including one previously published replicate for each species (11). We primarily focused on the comparison of cell types and gene expression between these two species of common interest (9, 11, 22, 23). We also included one sample each for *D. santomea* and *D. teissieri* to provide a general perspective of cell type conservation across species and phylogenetic context for gene expression changes we identified between *D. melanogaster* and *D. yakuba* (Fig. 1*A*). The mapping rates of sequencing reads to parental genomes were similar across samples and species (*SI Appendix*, Table S1). Immunostaining of *dsx*+ neurons revealed an average of ~735 *dsx*+ neurons in adult males (*D. melanogaster*: ~770; *D. yakuba*: ~700; see *SI Appendix,* Table S2), leading to an estimated 64× cellular coverage across the dataset of 46,922 *dsx*+ neurons (*D. melanogaster*: 22×; *D. yakuba*: 26×; *D. santomea*: 7×; *D. teissieri*: 9×).

Starting with *D. melanogaster* scRNA-seq data, we performed an initial clustering with the goal of identifying previously defined *dsx*+ neuronal clusters (25), which we refer to as "parental clusters" (Fig. 1*A*). Upon identifying unique marker genes, we used a split-GAL4 genetic intersectional approach, pairing *dsx* hemidrivers with hemidrivers against marker genes for each parental cluster (26). This strategy, combined with previously known marker genes such as *Hox* genes, allowed us to validate the fidelity of the clustering and successfully assign parental cluster identities: aDN (*tey*+); pC1 (*Optix*+); pC2l (*TfAP-2*+, *tsh*–); pC2m (*sv*+); pCd-1 (*unc-4*+); pCd-2 (*Gad1*+); TN1 (*TfAP-2*+, *tsh*+); TN2 (*ara*+, *abd-A*–, *Abd-B*–), ANm (*abd-A*+ and/or *Abd-B*+) (*SI Appendix*, Fig. S1). We did not identify cell clusters corresponding to the single-neuron pairs pMN1, pMN3, pLN, and sLG and the TN2 single-neuron pairs prA, prC, msB (*ara* partially labeled TN2), which together comprise less than 2% of all *dsx*+ neurons. As these unidentified neurons exhibit larger soma, we speculate that they might be lost during sample preparation due to sensitivity to experimental procedures or cell sorting stringency. Based on the same marker genes, we defined the parental clusters in the other three species and used MetaNeighbor (27) to validate the assignment of homologous parental clusters across species (Fig. 1*B* and *SI Appendix*, Fig. S2). The high degree of species consensus justified the further integration of data from all the four species into one dataset for identifying and comparing cell types on a common clustering space (Fig. 1*A*). Overall, the marker genes for parental clusters were well conserved across species (Fig. 1*C*). The majority of the top 20 markers for each parental cluster in a species were also marker genes for the same cluster in the other three species (Fig. 1*D*).

To resolve the cellular diversity within each parental cluster, we extracted each parental cluster from the integrated dataset for subclustering. In total, we defined 84 subclusters that we refer to as cell types, by iteratively subdividing each parental cluster until further division no longer yielded strong marker genes (Fig. 2*A*). The aDN, pCd-2, and TN2 clusters resolved into 2, 3, and 6 subclusters, respectively, each likely representing a single-neuron pair, most distinguishable by a single marker gene (Fig. 2*B* and *SI Appendix,* Fig. S3). Larger parental clusters that likely derived from a single hemilineage origin, such as pC1 and pC2 (28)—whose heterogeneity is well appreciated but poorly understood—resolved into subclusters that typically represent a group of neurons (Fig. 2*B* and *SI Appendix,* Fig. S3). While some of these subclusters are distinguishable by a single marker (e.g., pC1_6), others are harder to define and accordingly display continuity in clustering space (Fig. 2 *A* and *B*). This continuity may reflect the biological nature of these cell types defined by the quantitative expression levels of multiple genes. As expected from its diverse hemilineage origins (29), the ANm cluster resolved into 50 discrete subclusters, many well-defined by a single marker gene (*SI Appendix,* Fig. S3). Based on described marker genes (29, 30), we were able to annotate the hemilineage origin for 25 ANm subclusters, spanning at least 16 hemilineages (*SI Appendix,* Fig. S4). Overall, these subcluster marker genes are largely shared across species (Fig. 2*C*), though to a lesser degree than those of the parental clusters (Fig. 1*D*). Unless stated otherwise, all subsequent analyses were conducted on these subclusters that represent molecularly distinct cell types at a fine-grained level.

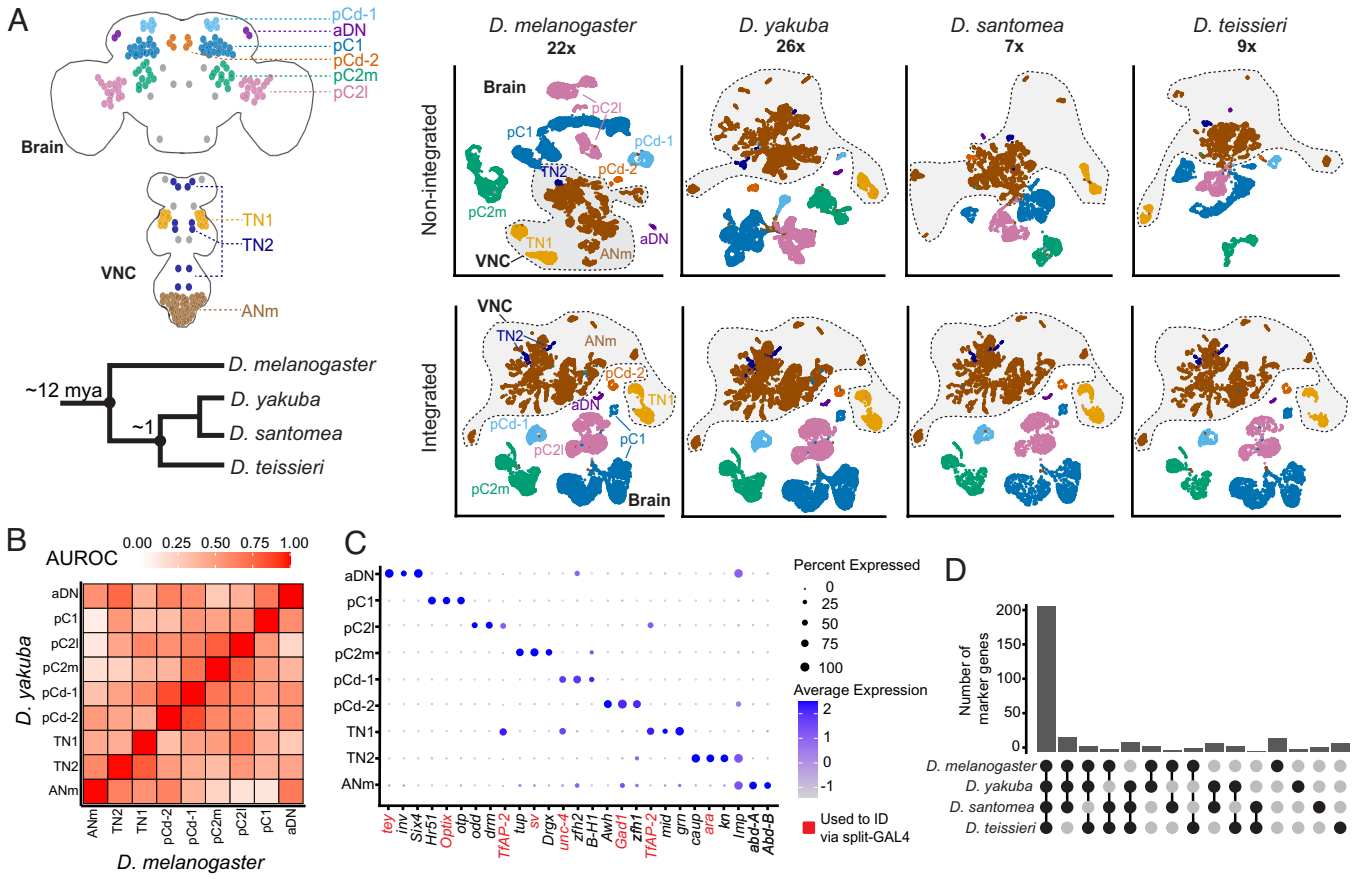

Fig. 1. Identification of parental clusters in scRNA-seq data in four species. (*A*) *Left*: schematic representation of the cell bodies of *dsx*+ neurons in the brain and VNC, color-coded by parental clusters, and a phylogeny of species included in this study. Gray dots represent *dsx*+ neurons that are not identified in our scRNA-seq data. *Right*: UMAP representations of scRNA-seq data from four species, color-coded to match the *dsx*+ parental clusters on the *Left*. The *Top* row shows single species (nonintegrated) data, while the *Bottom* row displays the integrated data separated by species. Estimates of cellular coverage (i.e., the average number of times each cell was sequenced) are noted for each species on top of the UMAPs. VNC clusters are outlined and shaded. (*B*) Heatmap showing the similarity (AUROC score) of parental clusters between *D. melanogaster* and *D. yakuba*. See *SI Appendix*, Fig. S2 for additional pairwise comparisons between species. (*C*) Dotplot illustrating the average expression and percentage of cells expressing three top marker genes for each parental cluster across the entire dataset. Genes highlighted in red were used to identify parental clusters via split-GAL4 (*SI Appendix*, Fig. S1). (*D*) Barplot displaying the number of marker genes conserved across species, including only the top 20 marker genes for each parental cluster for each species. Marker genes from all nine parental clusters are shown.

Overall Conservation of Fine-Grained *dsx*+ Cell Types across Four Species. Among the 84 molecularly distinct subclusters, 82 were found across all four species. The remaining two included TN1_4, corresponding to a TN1 subtype that we previously reported to contribute to the lineage-specific loss of sine song in *D. yakuba* males (11), and ANm_47, a small ANm cluster absent in *D. santomea*. We further examined species differences in the relative abundance of cell types between *D. melanogaster* and *D. yakuba*, where biological replicates were available. Based on the cell number of each *dsx*+ parental cluster quantified by immunostaining in both species (*SI Appendix*, Table S2), we normalized the subcluster cell counts by scaling the total number of cells in each parental cluster to its corresponding immunostaining estimate for that species. Using scCODA (31), we identified 12 species-biased subclusters that varied in cell number by 1.3- to 6.6-fold. Of these, ten were in the ANm (ANm_4/8/17/18/24/25/32/33/45/48, all *D. yakuba*-biased), and the other two were TN1_2 (*D. melanogaster*-biased) and pC1_6 (*D. yakuba*-biased) (Fig. 3). Given the high heterogeneity of cell types within the ANm cluster and the difficulty of accurately quantifying neurons in this densely packed region, the prevalent species differences in the ANm cluster should be interpreted with caution. Nevertheless, these subclusters are potential candidates for more variable cell types across species, warranting future validation and functional investigation. These results suggest that, even with the capability to resolve molecular cell types of single-neuron pairs, gains and losses of these fine-grained cell types are rare over 12 My of evolutionary divergence, whereas species differences in their relative abundance might be more prevalent.

Cell-Type-Specific Transcriptomic Conservation and Divergence across Species. Recent scRNA-seq comparisons suggest that the transcriptomes of some cell types have diverged more rapidly than others, potentially reflecting differences in evolutionary constraints and adaptive functional divergence (32, 33). For instance, neuronal cell types show pronounced transcriptomic divergence between nematode species (33). However, it remains unclear how transcriptomic conservation and divergence vary among individual neuronal cell types with similar or different functions. We addressed this question by comparing the transcriptomic correlations of *dsx*+ cell types between *D. melanogaster* and *D. yakuba* and examining technical and functional factors that may underlie these patterns. For each subcluster, we used Spearman rank correlation of gene expression to provide a continuous measure for the degree of transcriptomic conservation (34). Subclusters with higher scores indicate greater transcriptomic conservation, whereas those with lower scores indicate greater transcriptomic divergence. The correlation scores, ranging from 0.60 to 0.73, exhibit substantial

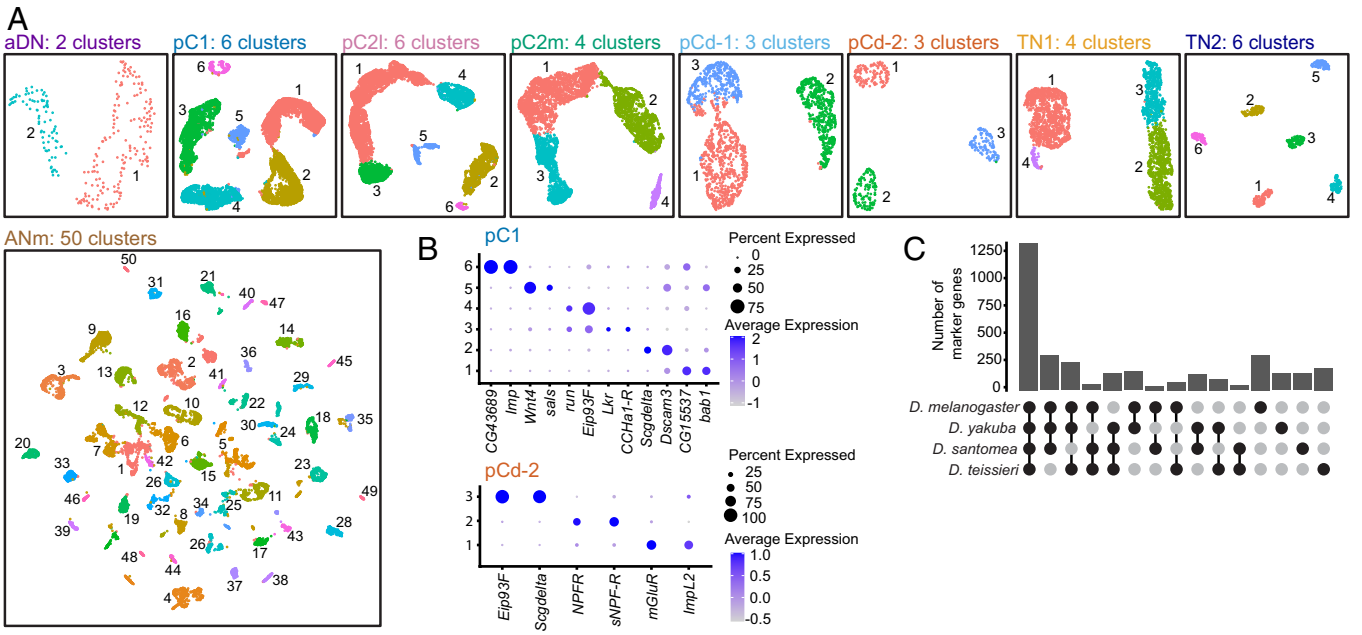

Fig. 2. Subclustering analyses of the parental clusters from the integrated four-species dataset. (*A*) UMAP representations of the subclustering of parental clusters. Different colors represent molecularly distinct cell types. (*B*) Representative dotplots showing the average expression and percentage of cells expressing two marker genes for each subcluster within pC1 (*Top*) and pCd-2 (*Bottom*). See *SI Appendix*, Fig. S3 for top marker genes for subclusters in other parental clusters. (*C*) Barplot displaying the number of marker genes conserved across species, including only the top 20 marker genes for each subcluster for each species. Marker genes from all subclusters are shown.

variation even among subclusters within the same parental cluster (Fig. 4*A*).

We examined whether the heterogeneity in transcriptomic correlation could be driven by possible technical characteristics. First, we tested whether the correlation score simply reflected how well the cell type can be molecularly defined. Cell types that are less well-defined might lead to misassignment of cell types, which may artificially lower correlation scores. To check this, we calculated the mean silhouette score (35), a measure of clustering quality, and found no association (*SI Appendix*, Fig. S5*A*). Similarly, the

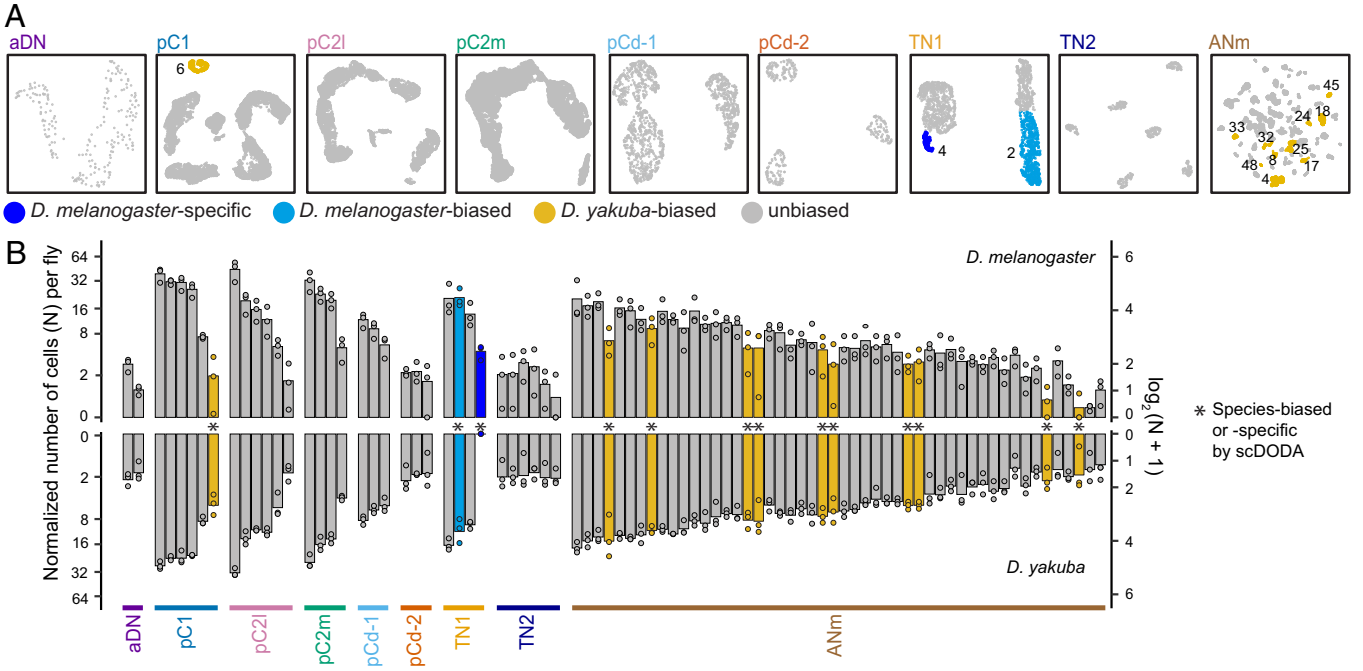

Fig. 3. Cell type number comparison between *D. melanogaster* and *D. yakuba*. (*A*) UMAP representations of the subclustering of parental clusters, color-coded by species differences in cell number within each subcluster. The identities of subclusters with significant species differences by scCODA are noted. (*B*) Barplot showing the number of cells (N) per fly in each subcluster, separated by species and grouped by parental cluster identity shown at the *Bottom*. For each subcluster in each species, cell numbers were normalized by scaling the total cell number of the corresponding parental cluster to the immunostaining estimate for that species (provided in *SI Appendix*, Table S2). Numbers are plotted on a $\log_2$ scale with an offset of 1 [$\log_2$ (N+1)] along the Y-axis to accommodate a wide range of values and to account for zeros.

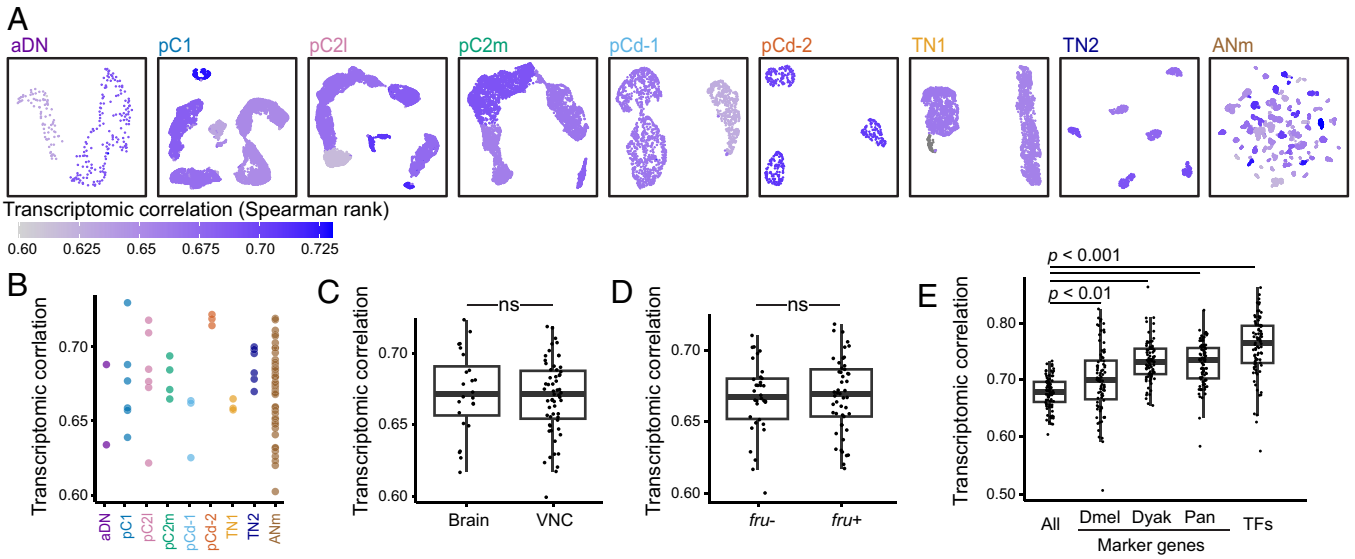

Fig. 4. Variation across subclusters in transcriptomic conservation between *D. melanogaster* and *D. yakuba*. (*A*) UMAP representations of the subclustering of parental clusters, color-coded by transcriptomic similarity between *D. melanogaster* and *D. yakuba* measured by Spearman rank correlation scores. (*B*) Transcriptomic correlation scores of subclusters grouped by parental cluster; no significant difference was observed across parental clusters (Kruskal–Wallis; $\chi 2 = 10.793$; $P = 0.213$). (*C*) Box and whisker plot showing transcriptomic correlation scores of subclusters grouped by central nervous system location, no significant difference was observed (*t* test; t = 0.486, df = 39.2, $P = 0.629$). (*D*) Box and whisker plot showing transcriptomic correlation scores grouped by whether or not the subcluster expresses *fru*, no significant difference was observed (*t* test; t = −0.4297, df = 72.6, $P = 0.767$). (*E*) Box and whisker plot showing transcriptomic correlation scores when including different sets of genes: all genes with median expression level greater than zero (All), marker genes identified from *D. melanogaster* data only (Dmel), marker genes from *D. yakuba* data only (Dyak), marker genes from the entire four-species dataset (Pan), and transcription factors (TFs) (ANOVA; F = 41.41, df = 4, $P < 0.001$).

correlation score was not associated with the number of cells in the subcluster (*SI Appendix,* Fig. S5*B*), or variability across replicates (*SI Appendix,* Fig. S5*C*). We did find a significant positive association with the number of genes expressed within a subcluster (*SI Appendix,* Fig. S5*D*), explaining 31.8% of the variance in the correlation scores among subclusters based on a generalized linear model. Randomly downsampling the gene set to the same number did not alter the association (Spearman r = 0.999, $P < 0.001$).

We further examined whether the heterogeneity could be explained by several functional characteristics. First, we asked whether cell types belonging to specific parental clusters are more conserved or divergent. While the variance of correlation scores across parental clusters was not homogeneous (Bartlett test; K2 = 16.482; $P = 0.0356$), pairwise Bartlett tests revealed no significant differences in variance between any two parental clusters. Further the nonparametric Kruskal–Wallis test showed that the correlation scores were not different among parental clusters (Fig. 4*B*). Second, the scores also did not differ between subclusters located in the brain versus the VNC (Fig. 4*C*). Finally, given that *fru* is a key transcription factor in the development and function of sexual circuits in males (14), we tested whether the scores varied as a function of *fru* gene expression and again found no difference (Fig. 4*D*).

Together, these analyses demonstrate that broad biological characteristics, including parental cluster identity, do not well account for the heterogeneity in transcriptomic divergence among fine-grained cell types, suggesting that the selective pressures shaping transcriptomic evolution are highly cell-type-specific. This sole correlation observed with the number of expressed genes raises the possibility that cell types with higher transcriptional activity may be more transcriptomically constrained. Additionally, these comparisons provided candidate circuit nodes with either constrained or divergent functions. The five most divergent subclusters (i.e., those with the lowest correlation scores) included four ANm subclusters (ANm_12/19/39/40) and pC2l_3. The five most conserved subclusters included three ANm subclusters (ANm_17/23/25), pC1_6, and pC2l_6. Notably, pC1_6 also appeared more abundant in *D. yakuba*, highlighting separable evolutionary modes of transcriptomic gene expression and cell type abundance.

Finally, we assessed how genes critical to cell identity contribute to transcriptomic conservation across species. Spearman rank correlations using only marker genes or only transcription factors yielded higher correlation scores, with the highest observed when using only transcription factors (Fig. 4*E*). These results suggest that genes essential for cell identity—particularly transcription factors—are subject to stronger evolutionary constraints on their expression.

Differential Gene Expression across Species Is Pervasive and Highly Cell-Type-Specific. Defining molecular cell types at high resolution provides an ideal framework for characterizing gene expression differences across species at the cell-type level, while also minimizing confounders arising from potential species differences in cell-type composition. Here, we identified differentially expressed genes (DEGs) for each subcluster between *D. melanogaster* and *D. yakuba*. Ambient RNA in single-cell suspensions can introduce contamination, leading to false-positive signals that appear as lowly expressed genes (36), artificially inflating the breadth of gene expression. Since fast-acting neurotransmitters typically show minimal cotransmission within a given cell type (37), we used the coexpression of their marker genes (*Gad1*, *VGlut*, and *VAChT*) as a proxy for potential ambient RNA contamination (30) to explore the optimal criterion of gene expression. When defining gene expression as nonzero read(s) in ≥10% of cells within a given subcluster, 20.2% (17 of 84) of subclusters appeared to release more than one neurotransmitter. In these cases, one neurotransmitter marker was expressed at a much higher level than the others, suggesting contamination. Alternatively, defining gene expression using a Bayesian mixture model by scMarco

(11, 26), where a gene is considered expressed if it has >50% probability of being detected, yielded results that aligned more closely with expectations: 82 of 84 subclusters were shown to release at least one fast-acting neurotransmitter, with only two subclusters releasing more than one neurotransmitter, indicating limited false-negatives and false-positives. Using this approach to filter out genes that were not expressed in either species with a relatively stringent threshold of a log fold change of three and a corrected *P*-value below 0.05 to identify credible candidates, 504 genes are DEGs in at least one subcluster (Dataset S1). These genes were mostly differentially expressed in a cell-type-specific manner, with many genes being differentially expressed in only a small subset of subclusters where they are expressed (Fig. 5*A*), regardless of whether they were sparsely or broadly expressed (Fig. 5*B*). To further evaluate the extent to which false positives from factors such as batch effect and stochastic gene expression may contribute to DEG identification, we performed DEG simulations under null and true conditions (see *SI Appendix*, *Methods* for details). On average, null simulations yielded only 6.45% of the number of DEGs detected in true simulations (P = 0.00553, *SI Appendix*, Fig. S6), indicating that false positives from these factors contribute little to the identified DEGs.

Conserved Sexual Identity Defined by *fru* Expression. Changes in the spatiotemporal regulation of sex determination genes are thought to be a major mechanism driving the evolution of sex-specific traits, with many examples reported in morphological adaptations (38–40). How often such processes occur in the nervous system and

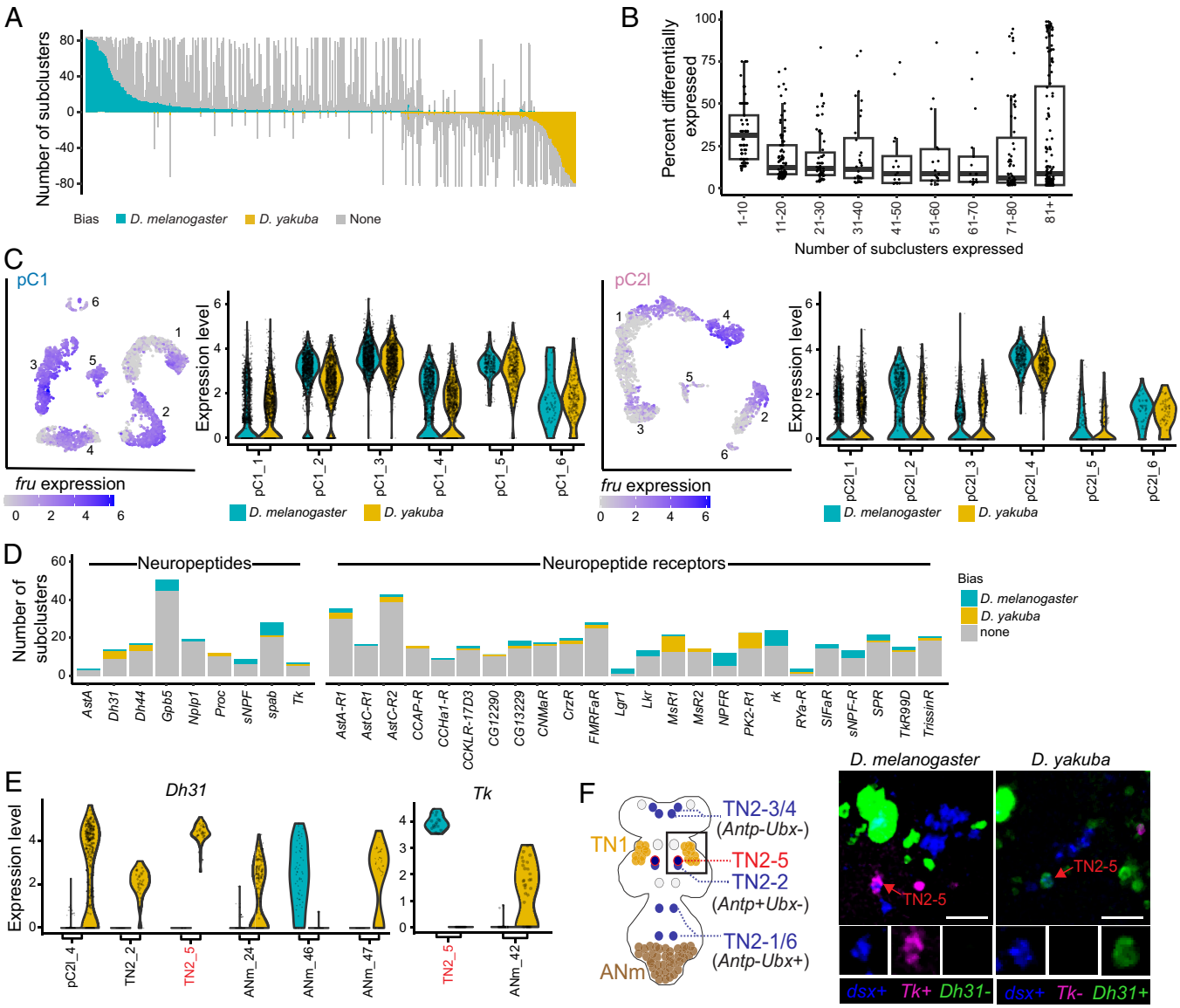

Fig. 5. DEG analyses between *D. melanogaster* and *D. yakuba*. (*A*) Barplot showing the number of subclusters in which a gene is expressed, color-coded by the number of those subclusters in which the gene is a DEG and the direction of species bias. Each bar represents a single gene. (*B*) Box and whisker plot showing the percentage of subclusters in which a gene is a DEG, binned by the number of subclusters in which the gene is expressed. (*C*) UMAP representations and violin plots showing the expression of *fru* in pC1 and pC2l subclusters. See *fru* expression in all *dsx*+ neurons across all four species in *SI Appendix*, Fig. S7. (*D*) Barplot showing DEGs of neuropeptides (*Left*) and neuropeptide receptors (*Right*), color-coded by the direction of species bias in the expressed subclusters. (*E*) Violin plots showing the expression levels of *Dh31* and *Tk* in both *D. melanogaster* and *D. yakuba* in all the subclusters where expression levels are significantly different between the two species. (*F*) Species differences in the gene expression patterns of *Dh31* and *Tk* in the TN2-5 cell type. *Left*: schematic denotes the cell body location of TN2-5 and the appropriate imaging region (open black box). *Right*: representative confocal images of in situ HCR against *dsx*, *Dh31*, and *Tk* mRNA. Images presented as maximum intensity projections of z-stacks covering the cell body of TN2-5. (Scale bar: 20 μm.) See UMAP representations of *Dh31* and *Tk* gene expression in TN2 neurons across all four species in *SI Appendix*, Fig. S10.

contribute to behavioral evolution remains unknown. Like *dsx*, the sex determination gene *fru* plays a central role in defining the sex-specific fate of neurons and acts as a master regulator of sexual circuit development and function (14). The *dsx*+ neurons include both *fru*+ and *fru*- populations with known functional differences (9, 21). For example, *fru*+ and *fru*- populations within the parental cluster pC1 exhibit behavioral specialization in courtship versus aggression (21) and distinct sensory responses to sexual pheromones (9). Consistent with *fru*'s prominent role in specifying cell fate, *fru* is a marker gene for 25 of the 84 subclusters, well above the average of 9.2 subclusters for all marker genes. Additionally, *fru* expression, both in presence/absence and quantitative levels, is highly spatially organized in UMAP space (Fig. 5*C* and *SI Appendix,* Fig. S7). While cell-type-specific changes in *fru* expression might seem like a plausible evolutionary mechanism for functional modifications, *fru* is not differentially expressed in any subcluster between *D. melanogaster* and *D. yakuba*, and its expression patterns are highly similar across all four species (Fig. 5*C* and *SI Appendix,* Fig. S7). Therefore, *fru*-specified sexual identity within *dsx*+ neurons is highly conserved across species, suggesting that the gain or loss of *fru* sexual identity may not be a frequent mode of evolutionary change in the nervous system.

Conserved Fast-Acting Neurotransmitter and Monoaminergic Identity. We annotated and compared subclusters that release the fast-acting neurotransmitters acetylcholine, GABA, and glutamate. Except for the highly diverse ANm clusters, all subclusters within each parental cluster shared the same neurotransmitter identity, which was conserved across all four species (*SI Appendix,* Fig. S8). Consistent with previous studies (41–43), pC1, pC2l, pC2m, pCd-1, TN1, and TN2 are cholinergic (*VAChT*/*VGAT*+), pCd-2 is GABAergic (*Gad1*+), and aDN is glutamatergic (*VGlut*+). Among the 50 ANm subclusters, 28 are cholinergic, 13 are GABAergic, seven are glutamatergic, and two lack expression of marker genes for these fast-acting neurotransmitters. Expression levels of these marker genes did not differ between *D. melanogaster* and *D. yakuba* in any subcluster. To annotate monoaminergic neurons, we used *Vmat*, which encodes a monoamine vesicular transporter, as a marker gene (44). Across all four species, *Vmat* is expressed in two ANm subclusters: ANm_14 is serotonergic (*SerT*+) and did not express maker genes of fast-acting neurotransmitters; and ANm_20 is dopaminergic (*DAT*+) (*SI Appendix,* Fig. S9). The serotonergic ANm_14 corresponds to a previously described neuron group that is necessary for successful copulation in *D. melanogaster* males (45). Expression levels of *Vmat*, *SerT,* and *DAT* did not differ between *D. melanogaster* and *D. yakuba*.

Rapid Evolutionary Turnover of Gene Expression in Neuropeptide Signaling Pathways. Neuropeptide signaling pathways, along with multiple terms related to synaptic connectivity and axon guidance, are among the enriched GO terms for DEGs. Here, we specifically focused on the expression patterns of neuropeptides and their receptors, given their important roles in regulating behaviors including sexual behaviors (46–52). Of the 23 neuropeptide genes expressed in at least one subcluster, nine are differentially expressed between *D. melanogaster* and *D. yakuba* in at least one subcluster (Fig. 5*D*). Three of these genes–*Dh31*, *Dh44*, and *Tk*–have been implicated in sexual behaviors, including male courtship (46–48, 52). Notably, all three genes are DEGs only in a subset of the subclusters where they are expressed, with expression biased toward *D. melanogaster* in some subclusters and toward *D. yakuba* in others. Of the 34 neuropeptide receptors expressed in at least one subcluster, 25 are differentially expressed in at least one subcluster, with 14 whose gene expressions are biased toward different species depending on the subcluster. These 25 genes include *CCKLR-17D3* and *SIFaR*, both of which play roles in male courtship (50, 51) and are DEGs in a small subset of expressed subclusters.

One notable difference is in the cell type TN2-5, which expresses the neuropeptide *Tk* in *D. melanogaster* and *Dh31* in *D. yakuba* (Fig. 5*E*). Based on molecular markers, we registered TN2-5 to one of the two mesothoracic TN2 neuron pairs previously referred to as MsA (25) (Fig. 5*F* and *SI Appendix,* Fig. S10). Using multiplexed in situ Hybridization Chain Reaction (HCR) (53, 54), we confirmed that one neuron pair was consistently *Tk*+ and *Dh31*- in *D. melanogaster* and *Tk*- and *Dh31*+ in *D. yakuba* (Fig. 5*F*). Further scRNA-seq comparisons across four species showed that *D. yakuba*, *D. santomea*, and *D. teissieri* shared the same *Tk*- and *Dh31*+ pattern in TN2-5 (*SI Appendix,* Fig. S10), suggesting that the shift in *Tk* and *Dh31* expression might have co-occurred at the divergence between *D. melanogaster* and the common ancestor of the other three species.

Defining Sex Differences of *dsx*+ Cell Types in *D. melanogaster*. While some *dsx*+ parental clusters are male-specific or more abundant in males, female *D. melanogaster* also has a few hundred *dsx*+ neurons (~560 neurons by our estimation; see *SI Appendix,* Table S2), many of which regulate key aspects of female sexual behaviors (14, 15). The diversity of *dsx*+ cell types in females and the sex differences in *dsx*+ cell types–particularly in the ANm, where the majority of *dsx*+ neurons are found in females, have not been systematically characterized. Therefore, we generated a scRNA-seq dataset of *dsx*+ neurons in adult female *D. melanogaster* to define and compare cell types between sexes. This dataset not only provides foundational knowledge of female sexual circuits and sexual dimorphism but also enables our further exploration of the relationship between species- and sex- differences (see next section).

The female data include 3,802 high quality *dsx*+ cells from adult female *D. melanogaster*, resulting in ~7× coverage. To avoid clustering bias due to the much larger size of male dataset, we downsampled male *D. melanogaster* data to match the cellular coverage of the female dataset and then integrated them to define sex-specific and sex-biased cell types. Because females and males share the marker genes of the same parental clusters (*SI Appendix*, Fig. S1), we used these genes to define parental clusters in the integrated male/female dataset. Consistent with previous studies (25), TN1 and TN2 are male-specific, while pC1, pC2l, and pC2m are male-biased (Fig. 6*A*). We further resolved cell types by subclustering and defined sex-specific and sex-biased cell types as those subclusters consisting of over 95% or 75% of cells from one sex, respectively. Among the 79 subclusters resolved, we classified 50 as sex-unbiased, 21 as male-specific, 5 as female-specific, and 3 as female-biased (Fig. 6 *B* and *C*). The majority (71.43%) of male-specific cell types are in the brain, whereas all female-specific and female-biased ones are in the ANm. These labels should be largely conserved across the four species here given the highly conserved sex differences in parental clusters (*SI Appendix,* Table S2).

Male-Specific *dsx*+ Cell Types Do Not Exhibit Greater Divergence between Species. Males and females may experience different fitness consequences from the same evolutionary changes in shared cell types (55). Under this model, sex-shared cell types may be more evolutionarily constrained than sex-specific ones. Additionally, male reproductive tissues may undergo faster evolutionary change as a result of sexual selection (6, 56). However, whether sexually dimorphic cell types, especially male-specific cell types, exhibit greater species divergence than sex-unbiased cell types has never

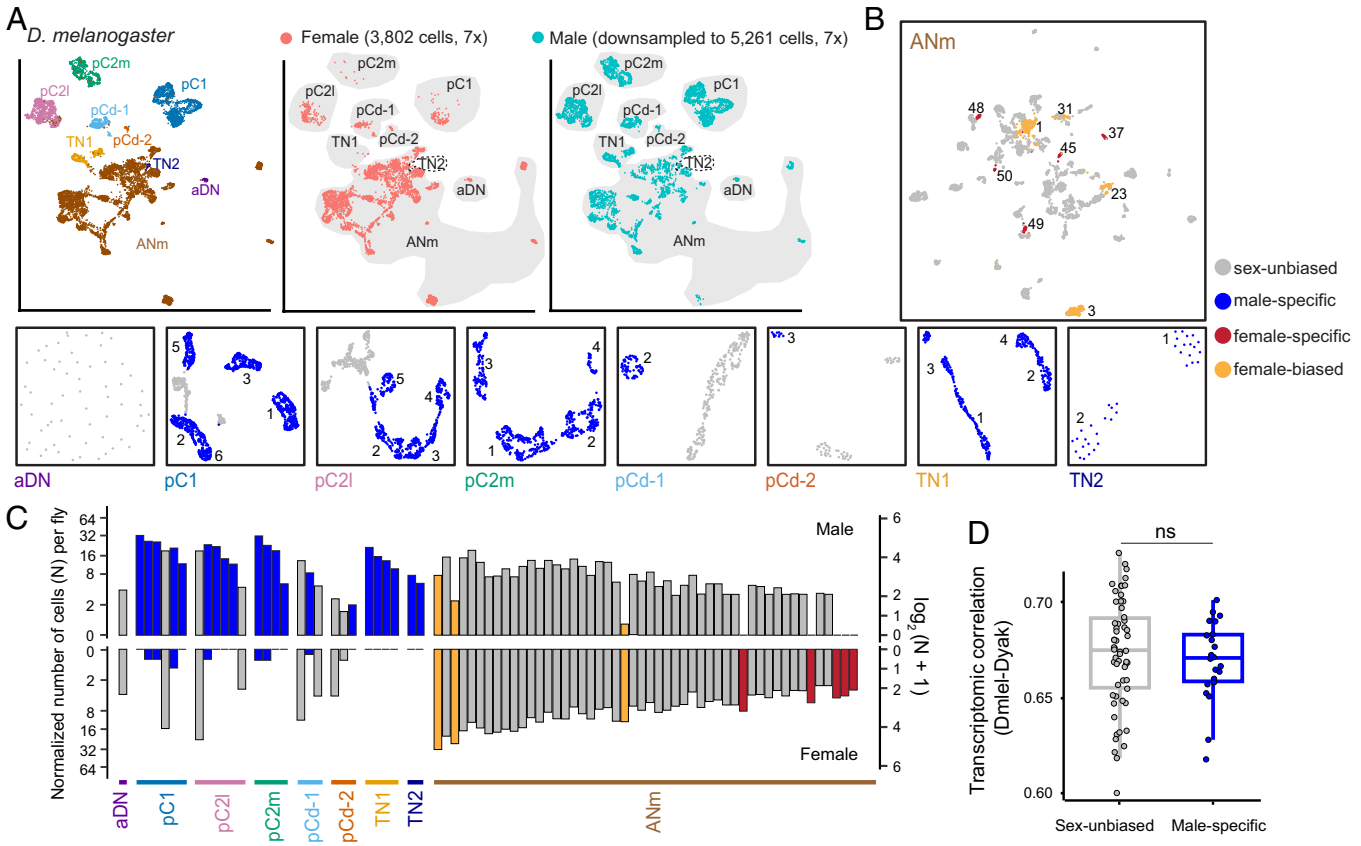

Fig. 6. Defining sex differences of *dsx*+ neurons in *D. melanogaster* and evolutionary comparison of *dsx*+ neurons by sex differences. (*A*) UMAP representations of integrated scRNA-seq data from the male/female dataset, with male cells downsampled to match the same 7× cellular coverage as the female data. (*B*) UMAP representations of the subclustering, color-coded by sex differences in cell number within each subcluster. The identities of subclusters with sex differences were noted. Refer to *SI Appendix*, Fig. S11*A* for the full annotation of subcluster identity. (*C*) Barplot showing the normalized number of cells (N) per fly in each subcluster, separated by sex, and color-coded by sex differences. For each subcluster in each sex, cell numbers were normalized by scaling the total cell number of the corresponding parental cluster to the immunostaining estimate for that sex (provided in *SI Appendix*, Table S2). Numbers are plotted on a $\log_2$ scale with an offset of 1 [$\log_2$ (N + 1)] along the Y-axis to accommodate a wide range of values and to account for zeros. (*D*) Box and whisker plot comparing transcriptomic correlation scores between *D. melanogaster* and *D. yakuba* (Dmel-Dyak) in four-species dataset for cell types grouped by sex differences. No significant difference was observed (*t* test; t = −0.671, df = 51.87, *P* = 0.505). See *SI Appendix*, Fig. S11*B* for a schematic example of transferring "sex-unbiased" and "male-specific" labels from the male/female dataset to the four-species male dataset.

been tested in the nervous system. The presence of male-specific and sex-unbiased cell types within *dsx*+ neurons provides a system to address this question.

To compare species divergence in relation to sex differences, first we have to transfer the "male-specific," and "sex-unbiased" labels from the male/female dataset to the four-species male dataset, by cross-referencing the cell type identities of male cells present in both datasets (*SI Appendix*, Fig. S11). Cells from 78 of the 84 subclusters found in the four species dataset were exclusively matched to either male-specific or sex-unbiased subclusters in the male/female dataset, allowing us to transfer these labels across datasets (*SI Appendix*, Table S3).

Upon label transfer, we tested whether male-specific cell types showed greater divergence between *D. melanogaster* and *D. yakuba* in relative abundance or transcriptomic patterns. Among the 21 male-specific cell types, three were either species-specific (TN1_4) or species-biased (pC1_6 and TN1_2), and one (pC2l_3) was among the five subclusters with the lowest transcriptomic correlation scores across species. However, male-specific cell types were not significantly overrepresented among species-specific or species-biased cell types (Fisher's exact test; odds ratio = 1.083; *P* = 1) or among those with the five lowest transcriptomic correlations (odds ratio = 1.248; *P* = 1). Furthermore, transcriptomic correlation scores did not differ among male-specific and sex-unbiased cell types (Fig. 6*D*). Therefore, contrary to classic predictions, we found no clear association between sex differences and species divergence.

Resources for Cell-Type-Specific Labeling and Gene Expression Inquiries. Gaining genetic access to discrete cell types is crucial for investigating the organization, function, and evolution of the nervous system. Exploiting our datasets across species and between sexes, we used scMarco–a graphical user interface that binarizes gene expression in scRNA-seq data using a Bayesian mixture model approach (26)–to identify optimal combinations of molecular markers for each cell type defined in the four-species dataset (Dataset S2). Each cell type can be uniquely defined by the combination of two to three marker genes including *dsx*. This approach informs genetic intersection strategies for cell-type-specific labeling and functional manipulations, a powerful technique that has been demonstrated successfully (11, 26, 29). For *D. melanogaster*, users can cross-reference these marker genes or gene pairs with the gene-specific split-GAL4 database to identify existing driver lines or design new lines for targeted genetic manipulations (26), and many split-GAL4 lines can be generated by simple genetic crosses (57). Users may further intersect the split-GAL4 with dsx^{FLP} (58) to achieve labeling specificity as needed. Furthermore, both the four-species and the male/female datasets are publicly accessible through a Shiny app (https://apps.yenchungchen.com/dsx_neurons), an interactive web portal to

identify and evaluate optimal molecular markers for cell types of interest and to query gene expression on UMAP spaces across cell types, species, and sexes. These resources will facilitate the development of cell-type-specific tools in *D. melanogaster* and across species.

Discussion

A prerequisite for understanding behavioral evolution is to decipher how changes in the molecular identity of cell types shape divergent circuit properties and behaviors. In this study, we generated a comprehensive cell type atlas of male *dsx*+ neurons across four species of *Drosophila* (Figs. 1 and 2). Our species comparison revealed key aspects of neural circuit evolution, including cell types, transcriptomic conservation, and gene expression (Figs. 3–5). We also generated a cell type atlas for *dsx*+ neurons in female *D. melanogaster*, defined sex differences of *dsx*+ cell types, and tested whether male-specific cell types exhibit distinct evolutionary patterns (Fig. 6). Finally, we systematically identified combinations of molecular markers that uniquely label each cell type, enabling precise cell-type-specific functional characterization in future studies.

Our study provided the previously lacking granularity in cell type evolution. We showed that the cell type composition of sexual circuits, neural circuits that encode some of the most rapidly evolving behaviors, is highly conserved. Among the 84 defined cell types, ranging from one to about 23 neurons per hemisphere, we identified all but two across all four *Drosophila* species. Although this result does not preclude the importance of cell type evolution in behavioral adaptation, as demonstrated by many studies (59) and our earlier finding that the loss of a *dsx*+ cell type contributed to courtship song evolution (11), our findings indicate that behavioral evolution primarily proceeds through changes in the abundance, morphology, and physiology of existing cell types. We note that the appropriate level of granularity in defining cell types is an open question (60, 61). While our dataset can resolve single-neuron pairs, morphologically and functionally distinct cell types may not be fully distinguishable at this molecular level, and additional cell types lacking strong marker genes may still be embedded in our dataset. We also note that clustering strategies, such as species included for data integration, may also influence the precise outcome of cell type identification. Regardless, our study provides a necessary baseline for investigating the cellular basis of behavioral evolution. The high-resolution datasets generated here also enable further applications tailored to specific research questions and cell types of interest, such as adjusting clustering parameters, analyzing unintegrated or differently integrated datasets, combining data from different developmental stages, and incorporating additional neuronal modalities such as anatomy from high-resolution light microscopy or EM connectomes (62, 63).

In contrast to the overall conservation of the presence or absence of cell types, we identified many candidate events of species differences in cell type abundance and widespread transcriptomic changes. At the transcriptional level, we observed substantial variation in transcriptomic conservation even among cell types within the same parental cluster. This heterogeneity also aligns with the cell-type-specificity of DEGs, most of which were differentially expressed in only a small subset of cell types across species. Furthermore, contrary to the prediction that male-specific cell types may evolve more rapidly due to reduced genetic constraints and stronger positive selection, they do not exhibit greater divergence between species compared to sex-unbiased cell types. The rapid evolution of male-specific cell types is likely counterbalanced by strong purifying selection to maintain their critical roles in male sexual behaviors. Moreover, evolutionary changes may be localized to a limited subset of these cell types, such that male-specific cell types as a whole do not show elevated divergence. Together, our findings suggest that cell types are highly modular evolutionary units, with selective pressures shaping their molecular evolution in a strongly heterogeneous manner.

At the level of individual cell types, our study revealed conserved and evolvable aspects of gene expression in sexual circuits. Surprisingly, despite long-standing appreciation of *cis*-regulatory changes of master regulators as key drivers of phenotypic evolution, *fru*–a central orchestrator of male sexual circuits (14)–did not stand out as an obvious player. Both the composition of *fru*+ and *fru*- populations in *dsx*+ neurons and the quantitative expression of *fru* across cell types appear highly conserved in *dsx*+ neurons. (We note that species differences in *fru* expression not examined here may exist). This observation aligns with recent work revealing a conserved functional subdivision of P1 neurons, a subset of pC1 neurons that acts as a core node of the male courtship circuit, by *fru* expression (9). In addition, the similarity of *dsx*+ cell types and the quantitative levels of *dsx* gene expression across species indicate that *dsx*-defined sexual identity is also conserved. Other conserved features include higher transcriptomic conservation of genes essential for cell identity (i.e., transcriptional factors and marker genes) and an identical pattern of neurotransmitter identity (i.e., fast-acting neurotransmitters and monoamines) across all *dsx*+ cell types in all four species. Thus, the widespread gene expression differences observed between *D. melanogaster* and *D. yakuba*–accounting for 10.2% of all genes expressed in the dataset–should arise disproportionately from genes outside these core properties. Particularly, genes involved in neuropeptide signaling, which are implicated in behavioral evolution (64), exhibit striking evolutionary turnover in their gene expression patterns in a cell-type-specific manner. This evolutionary lability converges with recent findings in nematodes (8) and deer mice (5), suggesting that it represents a fundamental feature of neural circuit evolution. Together, our study revealed a dynamic evolutionary landscape of widespread, cell-type-specific modifications built upon a largely conserved organization of sexual circuits in cell types, sexual identity, and neurotransmitter identity.

The profound molecular and functional diversity among neuronal cell types, combined with their highly cell-type-specific evolutionary trajectories, highlights the urgent need for cell-type-specific genetic tools. This need is especially critical for studying evolutionary changes, as meaningful interpretation is contingent on comparing truly homologous neurons or neuronal groups across species. While transferring GAL4 and split-GAL4 enhancer drivers that label specific neurons in *D. melanogaster* into closely related species has been a fruitful approach (2), this approach can be constrained by factors such as species differences in enhancer activity and the lack of well-characterized reagents in *D. melanogaster*. Unlike enhancer-based genetic tools, gene-specific tools that leverage native regulatory elements have been shown to reliably recapitulate the expression patterns of targeted genes (26). By identifying molecular markers and marker combinations that represent specific cell types, our efforts provide a roadmap for designing these essential tools within and across species.

Finally, we have uncovered many interesting evolutionary changes, inviting future validation and functional characterization. As a proof of principle, we validated that the single-neuron cell type TN2-5 has undergone an evolutionary switch in neuropeptide identity: expressing *Tk* in *D. melanogaster* and *Dh31* in *D. yakuba*. Although the function of TN2-5 remains uncharacterized due to the lack of genetic tools, its male specificity and

mesothoracic location suggest a potential role in male-specific wing behaviors, such as courtship song and agonistic song (20, 65). Interestingly, in *D. melanogaster*, *Tk* signaling suppresses courtship and enhances aggression (46, 52), while gut-derived *Dh31* signaling promotes courtship (48). Future research may uncover the behavioral role of TN2-5 and the phenotypic consequences of its evolutionary shift in neuropeptide identity, now made possible by identifying marker genes that enable cell-type-specific tools. Given the widespread evolutionary turnover in the neuropeptide signaling pathway, a broadly relevant question is whether the behavioral states associated with these genes have diverged across species, or whether gene–behavior associations remain conserved, with changes in gene expression repurposing the same cell type to regulate distinct behaviors.

In conclusion, by using *dsx* as a molecular handle, we characterized the cellular and molecular diversity of sexual circuits with unprecedented detail. Our findings provide fundamental insights into the evolutionary dynamics of neural circuits at the single-cell-type level and the neural mechanisms of behavioral adaptation.

Materials and Methods

Information is available in *SI Appendix*. Briefly, we collected *dsx*+ neurons by fluorescently sorting genetically labeled neurons (*dsx*-GAL4>nls::tdTomato) from adult males of *D. melanogaster*, *D. yakuba*, *D. santomea*, and *D. teissieri*, as well as adult females of *D. melanogaster*. The sorted neurons were subjected to 10× Genomics sequencing. Reads were mapped to the corresponding reference genomes using Cell Ranger, restricted to orthologous genes shared across all four species, for subsequent clustering and gene expression analyses primarily conducted with Seurat. We generated two integrated datasets: 1) a four-species dataset comprising *dsx*+ male neurons from all four species, and 2) a male/female dataset containing both male and female *dsx*+ neurons from *D. melanogaster*.

Data, Materials, and Software Availability. Raw scRNA-seq data and the related R objects (.Rds files containing clustering results, metadata, and gene expression data) are available on Dryad under DOI: https://doi.org/10.5061/dryad.f4qrfj78h (66). The shiny app can be accessed via https://apps.yenchungchen.com/dsx_neurons/.

ACKNOWLEDGMENTS. We thank Lihua Li and Hongjie Li for their valuable input during the development of our scRNA-seq pipeline. We thank Troy Shirangi's lab for contributing to the sample dissection. We thank Nancy Zhang for valuable feedback on statistical methods and Yuan Chen for input on computational pipelines. We are immensely grateful for the generosity of the fly research community. Particularly, we thank Haluk Lacin, Yufeng Pan, Chris Doe, Gary Struhl, Joshua Kavaler, Nobert Perrimon, Ben Ewen-Campen, Ruth Lehmann, and Jing Wang for generously sharing genetic reagents and antibodies of marker genes. Although many experiments using these resources were not directly presented here, they have greatly informed our initial identification of *dsx*+ parental clusters before we took a split-GAL4 strategy for final validation. We thank Rory Coleman, Troy Shirangi, Stephen Goodwin, Megan Goodwin, and Aaron Allen for helpful comments on the manuscript. We thank John Murray and Michael Hart for their helpful inputs. We thank Jennifer Jakubowski, Shifu Tian, and Andrew Morschauser for their help with FACS. We thank Molly Gallagher and Diana Slater at the Center for Applied Genomics at the Children's Hospital of Philadelphia's Research Institute for help with library preparation and sequencing. Y.D. was supported by NIH grant R35GM142678. Y.-C.C. was supported by New York University (MacCracken Fellowship), by a NYSTEM institutional training grant (Contract #C322560GG), and by a Scholarship to Study Abroad from the Ministry of Education, Taiwan. Y.-C.D.C. is supported by the NIH National Eye Institute (K99EY035757).

Author affiliations: [a]Department of Biology, University of Pennsylvania, Philadelphia, PA 19096; and [b]Department of Biology, New York University, New York, NY 10003

Author contributions: J.T.W. and Y.D. designed research; J.T.W., I.P.J., H.G., and Y.D. performed research; Y.-C.D.C., Y.-C.C., and Y.D. contributed new reagents/analytic tools; J.T.W., D.S.C., and Y.D. analyzed data; and J.T.W. and Y.D. wrote the paper.

1. P. S. Katz, Neural mechanisms underlying the evolvability of behaviour. *Philos. Trans. R. Soc. Lond. B Biol. Sci.* **366**, 2086–2099 (2011).
2. R. J. V. Roberts, S. Pop, L. L. Prieto-Godino, Evolution of central neural circuits: State of the art and perspectives. *Nat. Rev. Neurosci.* **23**, 725–743 (2022).
3. J. Woych *et al.*, Cell-type profiling in salamanders identifies innovations in vertebrate forebrain evolution. *Science* **377**, eabp9186 (2022).
4. N. L. Jorstad *et al.*, Comparative transcriptomics reveals human-specific cortical features. *Science* **382**, eade9516 (2023).
5. J. Chen, P. R. Richardson, C. Kirby, S. R. Eddy, H. E. Hoekstra, Cellular evolution of the hypothalamic preoptic area of behaviorally divergent deer mice. *Elife* **13**, RP103109 (2025).
6. D. Lee, M. P. Shahandeh, L. Abuin, R. Benton, Comparative single-cell transcriptomic atlases of drosophilid brains suggest glial evolution during ecological adaptation. *PLoS Biol.* **23**, e3003120 (2025).
7. P. S. Katz, R. M. Harris-Warrick, The evolution of neuronal circuits underlying species-specific behavior. *Curr. Opin. Neurobiol.* **9**, 628–633 (1999).
8. I. A. Toker *et al.*, Divergence in neuronal signaling pathways despite conserved neuronal identity among Caenorhabditis species. *Curr. Biol.* **35**, 2927–2945.e7 (2025).
9. R. T. Coleman *et al.*, A modular circuit coordinates the diversification of courtship strategies. *Nature* **635**, 142–150 (2024).
10. M. Li *et al.*, Ancestral neural circuits potentiate the origin of a female sexual behavior in Drosophila. *Nat. Commun.* **15**, 9210 (2024).
11. D. Ye, J. T. Walsh, I. P. Junker, Y. Ding, Changes in the cellular makeup of motor patterning circuits drive courtship song evolution in Drosophila. *Curr. Biol.* **34**, 2319–2329.e6 (2024).
12. M. Capek *et al.*, Evolution of temperature preference in flies of the genus Drosophila. *Nature* **641**, 447–455 (2025).
13. B. R. Dürr *et al.*, Olfactory projection neuron rewiring in the brain of an ecological specialist. *Cell Rep.* **44**, 115615 (2025).
14. S. F. Goodwin, O. Hobert, Molecular mechanisms of sexually dimorphic nervous system patterning in flies and worms. *Annu. Rev. Cell Dev. Biol.* **37**, 519–547 (2021).
15. M. Oren-Suissa, T. R. Shirangi, Neural circuits underlying sexually dimorphic innate behaviors. *Annu. Rev. Neurosci.* **48**, 191–210 (2025).
16. H. T. Spieth, Courtship behavior in Drosophila. *Annu. Rev. Entomol.* **19**, 385–405 (1974).
17. R. J. Greenspan, J.-F. Ferveur, Courtship in Drosophila. *Annu. Rev. Genet.* **34**, 205–232 (2000).
18. R. R. H. Anholt, P. O'Grady, M. F. Wolfner, S. T. Harbison, Evolution of reproductive behavior. *Genetics* **214**, 49–73 (2020).
19. T. R. Shirangi, A. M. Wong, J. W. Truman, D. L. Stern, Doublesex regulates the connectivity of a neural circuit controlling Drosophila male courtship song. *Dev. Cell* **37**, 533–544 (2016).
20. T. Hindmarsh Sten, R. Li, F. Hollunder, S. Eleazer, V. Ruta, Male-male interactions shape mate selection in Drosophila. *Cell* **188**, 1486–1503.e25 (2025).
21. M. Koganezawa, K.-I. Kimura, D. Yamamoto, The neural circuitry that functions as a switch for courtship versus aggression in Drosophila males. *Curr. Biol.* **26**, 1395–1403 (2016).
22. D. L. Stern *et al.*, Genetic and transgenic reagents for Drosophila simulans, D. mauritiana, D. yakuba, D. santomea, and D. virilis. *G3 (Bethesda)* **7**, 1339–1347 (2017).
23. Y. Ding *et al.*, Neural evolution of context-dependent fly song. *Curr. Biol.* **29**, 1089–1099.e7 (2019).
24. A. Suvorov *et al.*, Widespread introgression across a phylogeny of 155 Drosophila genomes. *Curr. Biol.* **32**, 111–123.e5 (2022).
25. C. C. Robinett, A. G. Vaughan, J.-M. Knapp, B. S. Baker, Sex and the single cell. Part II. There is a time and place for sex. *PLoS Biol.* **8**, e1000365 (2010).
26. Y.-C. D. Chen *et al.*, Using single-cell RNA sequencing to generate predictive cell-type-specific split-GAL4 reagents throughout development. *Proc. Natl. Acad. Sci. U.S.A.* **120**, e2307451120 (2023).
27. M. Crow, A. Paul, S. Ballouz, Z. J. Huang, J. Gillis, Characterizing the replicability of cell types defined by single cell RNA-sequencing data using metaneighbor. *Nat. Commun.* **9**, 884 (2018).
28. Q. Ren, T. Awasaki, Y.-F. Huang, Z. Liu, T. Lee, Cell class-lineage analysis reveals sexually dimorphic lineage compositions in the Drosophila brain. *Curr. Biol.* **26**, 2583–2593 (2016).
29. J. H. M. Soffers *et al.*, A library of lineage-specific driver lines connects developing neuronal circuits to behavior in the Drosophila ventral nerve cord. *Elife* **14**, RP106042 (2025).
30. A. M. Allen *et al.*, A single-cell transcriptomic atlas of the adult Drosophila ventral nerve cord. *Elife* **9**, e54074 (2020).
31. M. Buettner, J. Ostner, C. L. Mueller, F. J. Theis, B. Schubert, ScCODA is a Bayesian model for compositional single-cell data analysis. *Nat. Commun.* **12**, 6876 (2021).
32. B. Guillotin *et al.*, A pan-grass transcriptome reveals patterns of cellular divergence in crops. *Nature* **617**, 785–791 (2023).
33. C. R. L. Large *et al.*, Lineage-resolved analysis of embryonic gene expression evolution in C. elegans and C. briggsae. *Science* **388**, eadu8249 (2025).
34. M. A. Skinnider, J. W. Squair, L. J. Foster, Evaluating measures of association for single-cell transcriptomics. *Nat. Methods* **16**, 381–386 (2019).
35. M. Tang *et al.*, Evaluating single-cell cluster stability using the Jaccard similarity index. *Bioinformatics* **37**, 2212–2214 (2021).
36. E. Caglayan, Y. Liu, G. Konopka, Neuronal ambient RNA contamination causes misinterpreted and masked cell types in brain single-nuclei datasets. *Neuron* **110**, 4043–4056 (2022).
37. F. P. Davis *et al.*, A genetic, genomic, and computational resource for exploring neural circuit function. *Elife* **9**, e50901 (2020).
38. T. M. Williams *et al.*, The regulation and evolution of a genetic switch controlling sexually dimorphic traits in Drosophila. *Cell* **134**, 610–623 (2008).
39. A. Kopp, Dmrt genes in the development and evolution of sexual dimorphism. *Trends Genet.* **28**, 175–184 (2012).
40. K. Kunte *et al.*, Doublesex is a mimicry supergene. *Nature* **507**, 229–232 (2014).
41. C. Zhou, Y. Rao, Y. Rao, A subset of octopaminergic neurons are important for Drosophila aggression. *Nat. Neurosci.* **11**, 1059–1067 (2008).
42. T. Nojima *et al.*, A sex-specific switch between visual and olfactory inputs underlies adaptive sex differences in behavior. *Curr. Biol.* **31**, 1175–1191.e6 (2021).

43. K. Imoto *et al.*, Neural-circuit basis of song preference learning in fruit flies. *iScience* **27**, 110266 (2024).
44. C. L. Greer *et al.*, A splice variant of the Drosophila vesicular monoamine transporter contains a conserved trafficking domain and functions in the storage of dopamine, serotonin, and octopamine. *J. Neurobiol.* **64**, 239–258 (2005).
45. Y. B. Yilmazer, M. Koganezawa, K. Sato, J. Xu, D. Yamamoto, Serotonergic neuronal death and concomitant serotonin deficiency curb copulation ability of Drosophila platonic mutants. *Nat. Commun.* **7**, 13792 (2016).
46. K. Asahina *et al.*, Tachykinin-expressing neurons control male-specific aggressive arousal in Drosophila. *Cell* **156**, 221–235 (2014).
47. X. Jiang, M. Sun, J. Chen, Y. Pan, Sex-specific and state-dependent neuromodulation regulates male and female locomotion and sexual behaviors. *Research* **7**, 0321 (2024).
48. H.-H. Lin *et al.*, A nutrient-specific gut hormone arbitrates between courtship and feeding. *Nature* **602**, 632–638 (2022).
49. S. M. Kim, C.-Y. Su, J. W. Wang, Neuromodulation of innate behaviors in Drosophila. *Annu. Rev. Neurosci.* **40**, 327–348 (2017).
50. S. Wu *et al.*, Drosulfakinin signaling in fruitless circuitry antagonizes P1 neurons to regulate sexual arousal in Drosophila. *Nat. Commun.* **10**, 4770 (2019).
51. A. Sellami, J. A. Veenstra, SIFamide acts on fruitless neurons to modulate sexual behavior in Drosophila melanogaster. *Peptides* **74**, 50–56 (2015).
52. S. Shankar *et al.*, The neuropeptide tachykinin is essential for pheromone detection in a gustatory neural circuit. *eLife* **4**, e06914 (2015).
53. H. M. Choi *et al.*, Third-generation in situ hybridization chain reaction: Multiplexed, quantitative, sensitive, versatile, robust. *Development* **145**, dev165753 (2018).
54. J. C. Duckhorn, I. P. Junker, Y. Ding, T. R. Shirangi, "Combined in situ hybridization chain reaction and immunostaining to visualize gene expression in whole-mount Drosophila central nervous systems" in *Behavioral Neurogenetics*, D. Yamamoto, Ed. (Springer, 2022), pp. 1–14.
55. T. Chapman, G. Arnqvist, J. Bangham, L. Rowe, Sexual conflict. *Trends Ecol. Evol.* **18**, 41–47 (2003).
56. H. Ellegren, J. Parsch, The evolution of sex-biased genes and sex-biased gene expression. *Nat. Rev. Genet.* **8**, 689–698 (2007).
57. S. A. Li, H. G. Li, N. Shoji, C. Desplan, Y.-C. D. Chen, Protocol for replacing coding intronic MiMIC and CRIMIC lines with T2A-split-GAL4 lines in Drosophila using genetic crosses. *STAR Protoc.* **4**, 102706 (2023).
58. C. Rezával *et al.*, Activation of latent courtship circuitry in the brain of Drosophila females induces male-like behaviors. *Curr. Biol.* **26**, 2508 (2016).
59. N. Konstantinides, C. Desplan, Neuronal circuit evolution: From development to structure and adaptive significance. *Cold Spring Harb. Perspect. Biol.* **17**, a041493 (2025).
60. H. Zeng, What is a cell type and how to define it? *Cell* **185**, 2739–2755 (2022).
61. M. N. Özel, C. Desplan, Does a cell's gene expression always reflect its function? *Nature* **638**, 899–900 (2025).
62. J. L. Lillvis *et al.*, Rapid reconstruction of neural circuits using tissue expansion and light sheet microscopy. *eLife* **11**, e81248 (2022).
63. D. Deutsch *et al.*, Sexually-dimorphic neurons in the Drosophila whole-brain connectome. bioRxiv [Preprint] (2025). https://doi.org/10.1101/2025.06.10.658788 (Accessed 6 October 2025).
64. L. F. Sullivan, M. S. Barker, P. C. Felix, R. Q. Vuong, B. H. White, Neuromodulation and the toolkit for behavioural evolution: Can ecdysis shed light on an old problem? *FEBS J.* **291**, 1049–1079 (2024).
65. T. Jonsson, E. A. Kravitz, R. Heinrich, Sound production during agonistic behavior of male Drosophila melanogaster. *Fly* **5**, 29–38 (2011).
66. J. Walsh, Y. Ding, Data from: High-resolution single-cell analyses reveal evolutionary constraints and evolvability of sexual circuits in Drosophila. Dryad. https://doi.org/10.5061/dryad.f4qrfj78h. Deposited 20 October 2025.